Research of Model Matching Control of Torque Vectoring Differential Gear System

Yutaka Hirano [1]

[1]Toyota Motor Corporation, Japan, yutaka_hirano@mail.toyota.co.jp

Abstract

In this paper, model-based development of a control of torque vectoring differential (TVD) gear system is described. A new control logic was developed using model matching control to let the vehicle yaw rate and vehicle slip angle follow the desired dynamics. Simulation results using a single track model of vehicle dynamics are shown to prove the efficacy of the proposed control. Modelica was useful to express time-varying state space system such as the single track model of vehicle dynamics. Also full vehicle model considering all of the vehicle dynamics and drive train motion using Modelica clarified the characteristics of this method in actual driving cases.

Keywords: Model Based System Development, Vehicle Dynamics, Torque Vectoring, Model Matching Control

1 Introduction

To satisfy needs for future low-carbon mobility society, development of many new electric vehicles (EVs) is increasingly active in recent years. Additionally many new proposals about integrated electric power train which also has torque vectoring capability are presented. Authors had made an integrated model of the total vehicle system of such an EV using Modelica (Hirano, 2014) (Hirano, 2015).

In the paper (Hirano, 2014), the authors showed the capability of new construction of the new EV using new type of tire based on 'Large and Narrow concept' and torque vectoring differential (TVD) gear. For the model based development of the new EV, various kind of running resistance, vehicle dynamic performance and proper design of electric regeneration system were studied. In another previous research (Hirano, 2015), a multi-physics full vehicle model of the new EV is expanded to consider the detailed loss of motors and inverters. Also front and rear suspension model which has same 3D mechanical design as the real experimental vehicle was made and verified. By technical investigations using this full vehicle model, structure, specifications and control of the new EV system were researched about vehicle dynamics and energy consumption. However, the control logic of the TVD gear was only simple PI feedback control in the previous papers. In this paper, model based control of TVD gear system is developed using model matching control technique. Single track model of vehicle dynamics is used to derive and verify the new control. At the same time, detailed design parameter of vehicle dynamics was obtained from the analysis of Modelica full vehicle model using detailed suspension model. Finally the developed controls were verified by using both the single track model and the full vehicle model.

2 Specification of Experimental EV

Table 1. Specifications of new experimental EV

	New EV	Conventional car
Vehicle Weight	750 kg	1240 kg
Yaw Moment Inertia	869 kgm^2	2104 kgm^2
Wheelbase	2.6 m	2.6 m
Front : Rear Weight Distribution	0.48 : 0.52	0.62 : 0.38
Height of CG	0.38 m	0.55 m
Aerodynamic Drag × Frontal Area	0.392 m^2	0.644 m^2
Tire RRC	5×10^{-3}	8.8×10^{-3}
Tire Normalized CP	16.1	20.4

The proposed experimental EV has specifications as shown in Table 1 (Hirano, 2015). Compared with a conventional small-class passenger car, the new EV has characteristics of lighter vehicle weight, smaller yaw moment of inertia, lower height of the center of gravity (CG) and lower rolling resistance coefficients (RRC) of tires. Because of these characteristics, this new EV is expected to have better handling and lower energy consumption than conventional vehicles. On the other hand, because of lighter weight and lower value of tire normalized CP (Cornering Power), this new EV seems more sensitive against external disturbances such as crosswind and road irregularity than the conventional cars. To cope with this problem, direct yaw moment control (DYC) was applied by using a new integrated transaxle unit for rear axle which has a main electric motor and also TVD gear unit with a control motor.

3 Vehicle Model for Controller Design

3.1 Single Track Vehicle Model

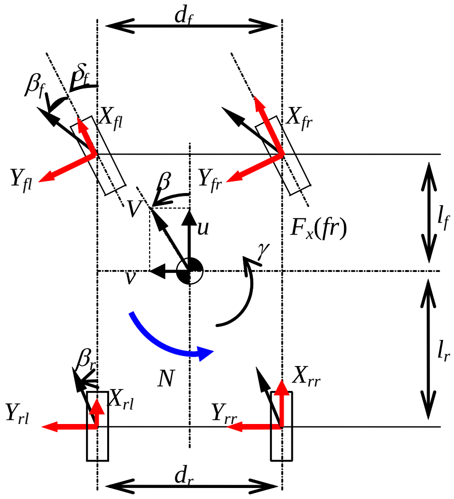

Figure 1. Expanded single track vehicle model

Figure 1 shows an expanded single track vehicle dynamics model to derive the control logic. The simplified equations of motion by this model become as follows.

$$M\frac{dV}{dt} = F \approx (X_{fr} + X_{fl})\cos\delta_f + (X_{rr} + X_{rl}) \quad (1)$$

$$M\frac{d}{dt}\left(V\tan^{-1}\beta + V\gamma\right) \approx Y_{fl} + Y_{fr} + Y_{rl} + Y_{rr} \quad (2)$$

$$I_z\frac{d\gamma}{dt} \approx l_f(Y_{fl} + Y_{fr})\cos\delta_f - l_r(Y_{rl} + Y_{rr}) + N \quad (3)$$

$$N = d_f(X_{fr} - X_{fl})\cos\delta_f + d_r(X_{rr} - X_{rl}) \quad (4)$$

Here,

- β : Vehicle slip angle,
- γ : Vehicle yaw rate,
- M : Vehicle mass,
- V : Vehicle velocity,
- I_z : Vehicle yaw moment of inertia,
- l_f (l_r) : Distance from the CG to front (rear) axle, (CG: Center of Gravity)
- d_f(d_r): Tread of front (rear) axle,
- X_{**} : Longitudinal force of each tire,
- Y_{**} : Lateral force of each tire,
- δ_f : Steering angle of front tire,
- F : Vehicle driving force,
- N : DYC moment by TVD.

3.2 Equation of Motion for Vehicle Dynamics

To derive the equations of motion for the target vehicle, equations (1) to (4) were further simplified. The lateral force at left and right tires were assumed to be equal and let $Y_{fl} = Y_{fr} = Y_f$, $Y_{rl} = Y_{rr} = Y_r$. Also we assume $\cos\delta_f \approx 1$ when front tire steering angle is not so big, and $\tan^{-1}\beta \approx \beta$ when β is small. Also by considering the TVD power unit is equipped only in the rear axle, the equations of motion become as follows.

$$M\frac{dV}{dt} = F = (X_{rr} + X_{rl}) \quad (5)$$

$$MV\left(\frac{d\beta}{dt} + \gamma\right) = 2Y_f + 2Y_r \quad (6)$$

$$I_z\frac{d\gamma}{dt} = 2l_fY_f - 2l_rY_r + N \quad (7)$$

where

$$Y_f = -K_f\beta_f = -K_f\left(\beta + \frac{l_f}{V}\gamma - \delta_f\right) \quad (8)$$

$$Y_r = -K_r\beta_r = -K_r\left(\beta - \frac{l_r}{V}\gamma\right) \quad (9)$$

$$N = d_r(X_{rr} - X_{rl}) \quad (10)$$

Here, K_f and K_r are the equivalent cornering power of front and rear tire respectively. These values are calculated by using the full-vehicle model described in the section 5.1 to consider the effects of elasticity and friction of suspension and steering.

If driving force F and DYC moment N can be calculated by some control logic, then the target longitudinal forces of left and right rear wheel to be realized by TVD power unit become as follows from equation (5) and equation (10).

$$X_{rr} = \frac{1}{2}\left(F + \frac{N}{d_r}\right) \quad (11)$$

$$X_{rl} = \frac{1}{2}\left(F - \frac{N}{d_r}\right) \quad (12)$$

3.3 Longitudinal Driving Force Controller

Let us suppose the desired value of vehicle speed, vehicle yaw rate and vehicle slip angle as V_{ref} , γ_{ref} and β_{ref} respectively.

The desired vehicle driving force F can be calculated as below by PI feedback control and equation (5).

$$F = M\frac{dV_{ref}}{dt} + K_{PF}(V_{ref} - V) + K_{IF}\int(V_{ref} - V)dt \quad (13)$$

Here K_{PF} is a proportional feedback gain and K_{IF} is an integral feedback gain.

3.4 Model Matching Controller of Lateral Dynamics

3.4.1 Dynamic Model of Vehicle Lateral Dynamics

For the lateral dynamics, the state space form of the vehicle dynamics with TVD control becomes as follow from equation (6) and (7).

DOI 10.3384/ecp1612415

$$\frac{d}{dt}\begin{bmatrix}\beta\\ \gamma\end{bmatrix}=\begin{bmatrix}-\frac{2(K_f+K_r)}{MV} & -1-\frac{2(l_fK_f-l_rK_r)}{MV^2}\\ -\frac{2(l_fK_f-l_rK_r)}{I_z} & -\frac{2(l_f{}^2K_f+l_r{}^2K_r)}{I_zV}\end{bmatrix}\begin{bmatrix}\beta\\ \gamma\end{bmatrix}+\begin{bmatrix}\frac{2K_f}{MV}\\ \frac{2l_fK_f}{I_z}\end{bmatrix}\frac{\delta_s}{G_s}+\begin{bmatrix}0\\ \frac{1}{I_z}\end{bmatrix}N \quad (14)$$

Here, $\delta_f = \delta_s/G_s$ (δ_s: steering wheel input angle, G_s: steering gear ratio).

Now the matrix form of the state space system of equation (14) can be written as follows.

$$\dot{x}=Ax+Bu+E\delta_s \quad (15)$$

$$x=\begin{bmatrix}\beta\\ \gamma\end{bmatrix},\qquad u=N$$

$$A=\begin{bmatrix}-\frac{2(K_f+K_r)}{MV} & -1-\frac{2(l_fK_f-l_rK_r)}{MV^2}\\ -\frac{2(l_fK_f-l_rK_r)}{I_z} & -\frac{2(l_f{}^2K_f+l_r{}^2K_r)}{I_zV}\end{bmatrix}=\begin{bmatrix}a_{11} & a_{12}\\ a_{21} & a_{22}\end{bmatrix} \quad (16)$$

$$B=\begin{bmatrix}0\\ \frac{1}{I_z}\end{bmatrix} \quad (17)$$

$$E=\begin{bmatrix}\frac{2K_f}{G_sMV}\\ \frac{2l_fK_f}{G_sI_z}\end{bmatrix} \quad (18)$$

Please note that the elements of the matrix A of the equation (15) as shown in the equation (16) are dependent on the vehicle velocity V, namely time-varying variables.

3.4.2 Desired Dynamics Model for Lateral Motion

The desired dynamics of vehicle yaw rate and vehicle slip angle are assumed as the first order lag function of steering wheel input as below.

$$x_d=\begin{bmatrix}\beta_{ref}\\ \gamma_{ref}\end{bmatrix}=\begin{bmatrix}\frac{k_\beta}{1+s\tau_\beta}G_{\beta 0}\\ \frac{k_\gamma}{1+s\tau_\gamma}G_{\gamma 0}\end{bmatrix}\delta_s \quad (19)$$

Here, $G_{\beta 0}$ and $G_{\gamma 0}$ are steady state gain of slip angle and yaw rate respectively from the steering input. k_β and k_γ are gain of desired slip angle and desired yaw rate from the steady state gain of each state variables. τ_β and τ_γ are time constant of desired slip angle and desired yaw rate as the first order lag function. Each state variables of slip angle and yaw rate at steady state can be calculated by solving the following equation

$$0=Ax_0+E\delta_s \quad (20)$$

and be obtained as follow.

$$x_0=-A^{-1}E\delta_s=-\frac{MI_zV^2}{4K_fK_r(l_f+l_r)^2-2MV^2(l_fK_f-l_rK_r)}\times\begin{bmatrix}-\frac{4K_fK_rl_r(l_f+l_r)}{MI_zV^2}+\frac{2l_fK_f}{I_z}\\ \frac{-4K_fK_r(l_f+l_r)}{MI_zV}\end{bmatrix}\frac{1}{G_s}\delta_s \quad (21)$$

Thus, $G_{\beta 0}$ and $G_{\gamma 0}$ can be calculated as follows.

$$\begin{bmatrix}G_{\beta 0}\\ G_{\gamma 0}\end{bmatrix}=-\frac{MI_zV^2}{4K_fK_r(l_f+l_r)^2-2MV^2(l_fK_f-l_rK_r)}\times\begin{bmatrix}-\frac{4K_fK_rl_r(l_f+l_r)}{MI_zV^2}+\frac{2l_fK_f}{I_z}\\ \frac{-4K_fK_r(l_f+l_r)}{MI_zV}\end{bmatrix}\frac{1}{G_s} \quad (22)$$

The state space form of the desired dynamics can be written as below from the equation (19).

$$\dot{x}_d=A_dx_d+E_d\delta_s \quad (23)$$

Here,

$$A_d=\begin{bmatrix}-\frac{1}{\tau_\beta} & 0\\ 0 & -\frac{1}{\tau_\gamma}\end{bmatrix}\text{ and}$$

$$E_d=\begin{bmatrix}\frac{k_\beta}{\tau_\beta}G_{\beta 0}\\ \frac{k_\gamma}{\tau_\gamma}G_{\gamma 0}\end{bmatrix}.$$

3.4.3 Model Matching Control of TVD

A state equation of the error between desired values and actual values of state variables can be obtained as below by subtracting equation (23) from equation (15).

$$\dot{e}=Ae+Bu+(A-A_d)x_d+(E-E_d)\delta_s \quad (24)$$

$$e=x-x_d$$

Let's assume the virtual control input U as below.

$$BU=Bu+(A-A_d)x_d+(E-E_d)\delta_s \quad (25)$$

Then the equation (24) can be transformed as below.

$$\dot{e}=Ae+BU \quad (26)$$

Now we can design the feedback control gain K as

$$U=-Ke \quad (27)$$

by using various linear control theories for the equation (26). Though, as mentioned above, the matrix A is time-varying and dependent on vehicle velocity. To cope with this problem, an analytical solution using pole placement technique was used. By combining equation (26) and equation (27), the following equation is obtained.

$$\dot{e} = Ae - BKe = (A - BK)e \tag{28}$$

If we specify the pole of the dynamic system of the error e of equation (28) as p_1 and p_2 (p_1, p_2 <0) and K = [k_1, k_2], following equation can be derived.

$$|sI - (A - BK)| = (s - p_1)(s - p_2) \tag{29}$$

Here, s is the Laplace operator and I is the unit matrix. Above equation can be rewritten as follow.

$$\left| s\begin{bmatrix} 1 & 0 \\ 0 & 1 \end{bmatrix} - \left(\begin{bmatrix} a_{11} & a_{12} \\ a_{21} & a_{22} \end{bmatrix} - \begin{bmatrix} 0 & 0 \\ \frac{k_1}{I_z} & \frac{k_2}{I_z} \end{bmatrix} \right) \right|$$

$$= s^2 - (a_{11} + a_{22} - \tfrac{k_2}{I_z})s + a_{11}(a_{22} - \tfrac{k_2}{I_z}) - a_{12}(a_{21} - \tfrac{k_1}{I_z})$$

$$= s^2 - (p_1 + p_2)s + p_1 p_2$$

Thus, the following simultaneous equation can be obtained.

$$\begin{cases} (a_{11} + a_{22} - \tfrac{k_2}{I_z}) = (p_1 + p_2) \\ a_{11}(a_{22} - \tfrac{k_2}{I_z}) - a_{12}(a_{21} - \tfrac{k_1}{I_z}) = p_1 p_2 \end{cases} \tag{30}$$

By solving the equation (30) analytically, we can obtain following solutions of k_1 and k_2.

$$k_2 = I_z(a_{11} + a_{22} - p_1 - p_2)$$
$$k_1 = I_z\left\{ \frac{p_1 p_2 + a_{11}(a_{11} - p_1 - p_2)}{a_{12}} + a_{21} \right\} \tag{31}$$

Please note that the above solution of K = [k_1, k_2] is also dependent on vehicle velocity. (See equation (16).)

Finally, from the equation (25), the following solution of u (= N) can be calculated.

$$u = B^{+}\{-BKe - (A - A_d)x_d - (E - E_d)\delta_s\} \tag{32}$$

Here, B^{+} is a quasi-inverse matrix of B, and consequently B^{+} = [0 I_z]. ($B^{+}B$ = 1.) Finally we obtain the following solution of u.

$$u = -Ke - B^{+}(A - A_d)x_d - B^{+}(E - E_d)\delta_s \tag{33}$$

It is understood from equation (33) that the control input of the model matching controller consists of a feedback term of the error between desired value and actual value of state variables and also feedforward terms evoked from desired state variables and also steering input.

Figure 2 shows a plot of the feedback gain k_1 and k_2 by pole placement (p_1 =-20, p_2 =-21) according to the vehicle velocity.

Though we used analytical solution using pole placement in this paper, it is also possible to design the feedback gain K by gain scheduling method using other linear control techniques according to the change of vehicle velocity.

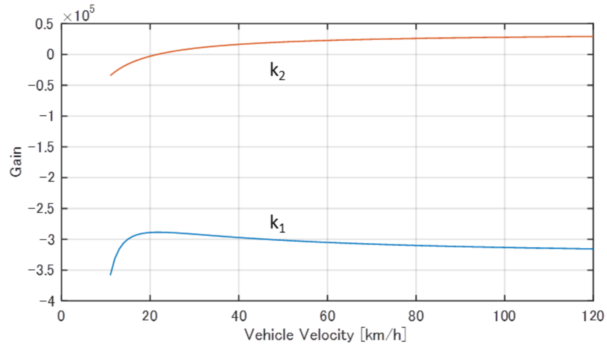

Figure 2 Plot of feedback gain by pole placement

4 Simulation Results by Single Track Vehicle Model

To confirm the validity of above mentioned model matching control, simulation test based on single track vehicle model was performed by using Modelica.

First of all, we should handle time-varying linear state space system such as that of equation (15) to (18). To cope with this problem, a new class of time-varying linear state space system was defined. To achieve this, the standard class of the state space system of Modelica Standard Library (MSL) was modified to release the constraint of variability of variables (i.e. by eliminating 'parameter' qualifier). The definition of the new class becomes as follow.

```
block StateSpace_Variable
…
extends Modelica.Blocks.Interfaces.MIMO(fi
nal nin=size(B, 2), final nout=size(C, 1));
  Real A[:, size(A, 1)];
  Real B[size(A, 1), :];
  Real C[:, size(A, 1)];
  Real D[size(C, 1), size(B, 2)]=zeros(siz
e(C, 1), size(B, 2)) ;
  output Real x[size(A, 1)](start=x_start)
 "State vector";
equation
  der(x) = A*x + B*u;
  y = C*x + D*u;
end StateSpace_Variable;


model SingleTrackModel
 …
  Real c0 = 2*(kf+kr);
  Real c1 = 2*(lf*kf-lr*kr);
  Real c2 = 2*(lf*lf*kf+lr*lr*kr);
…
 StateSpace_Variable Actual_x(
    A=A,
    B=B,
    C=identity(2));
 StateSpace_Variable Desired_xd(
    A=Ad,
    B=Ed,
    C=identity(2));
…
equation
  a11=-c0/m/v;
  a12=-1-c1/m/v/v;
```

```
  a21=-c1/iz;
  a22=-c2/iz/v;
  A={{a11, a12},
     {a21, a22}};
  B={{cf/m/v, 0},
     {cf*lf/iz, 1/iz}};
  Gb0=-m*iz*v*v/(cf*cr*l*l-m*v*v*c1)*(-
cf*cr*lr*l/m/iz/v/v + lf*cf/iz);
  Gr0=-m*iz*v*v/(cf*cr*l*l-m*v*v*c1)*(-
cf*cr*l/m/iz/v);
  Ad={{-1/t_b, 0},
      {0, -1/t_r}};
  Ed={{k_b*Gb0/t_b},
      {k_r*Gr0/t_r}};
  …
end SingleTrackModel;
```

For comparison, the definition of the standard class of the state space system in MSL is as below.

```
block StateSpace "Linear state space syste
m"
…
  parameter Real A[:, size(A, 1)]=[1, 0; 0
, 1];
  parameter Real B[size(A, 1), :]=[1; 1];
  parameter Real C[:, size(A, 1)]=[1, 1];
  parameter Real D[size(C, 1), size(B, 2)]
=zeros(size(C, 1), size(B, 2)) ;
…
equation
  der(x) = A*x + B*u;
  y = C*x + D*u;
  …
end StateSpace;
```

Also a new class of time-varying matrix gain to express the feedback gain by the equation (31) can be made by similar way.

Figure 3 shows a diagram of an example of a single track vehicle model combined with the desired vehicle dynamics model and the model matching controller.

Figure 4 shows a plot of vehicle speed and steering angle input used in the simulation by single track model. The vehicle accelerates from 10km /h to 100km/h between time 1 sec to 10sec. The steering angle moves as 1Hz sinusoidal curve. For comparison, simple PI feedback of desired yaw rate and that of desired slip angle were also tested. The control law of both PI controllers became as follows respectively.

PI feedback of desired yaw rate:

$$N = K_{P\gamma}(\gamma_{ref} - \gamma) + K_{I\gamma}\int(\gamma_{ref} - \gamma)dt \tag{34}$$

PI feedback of desired slip angle:

$$N = K_{P\beta}(\beta_{ref} - \beta) + K_{I\beta}\int(\beta_{ref} - \beta)dt \tag{35}$$

Desired dynamics was settled as k_β = 0.3, k_γ= 1.0. τ_β and τ_γ are settled as corresponding value of cut-off frequency of 1.3 Hz as shown in the equation (19).

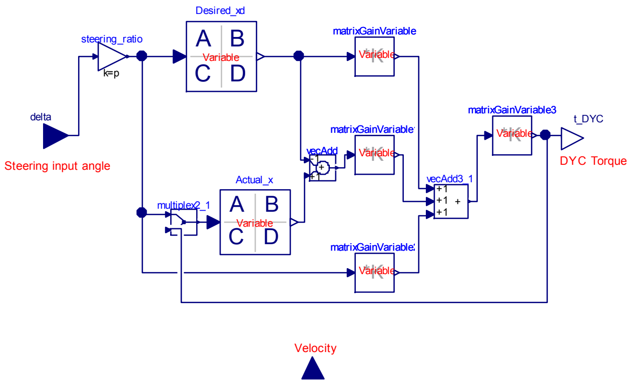

Figure 3. Modelica model of a single track model of vehicle and a controller

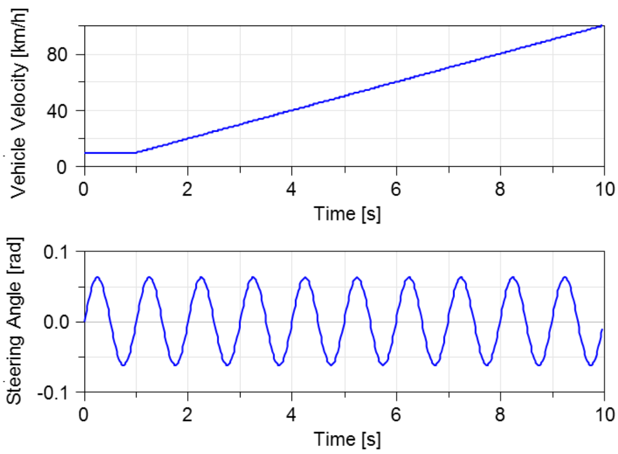

Figure 4. Plot of vehicle velocity and steering angle input

Figure 5 shows comparison of each control. The model matching control showed the best tracking performance of desired slip angle and desired yaw rate. Though, the control input N was bigger than other controls and also the tracking error of yaw rate was bigger especially at the low vehicle speed. Also, it was impossible to let both of the vehicle slip angle and the yaw rate to exactly track the desired value simultaneously. This is because that there are two independent state variables while there is only one control input.

Robustness of the model matching control (MMC) was also checked. **Figure 6** shows comparison of the simulation results of single track model when there are perturbation for the vehicle mass M and tire cornering power CP. For comparison, the result of yaw rate feedback control is also overlaid. MMC showed a good robustness against such parameter perturbations.

It is of course necessary to check the robustness of the control when parameter error of the plant and also other additional effects such as non-linearity and losses exist in the actual world. To do this, simulation tests using full vehicle model was also done as mentioned in the following section.

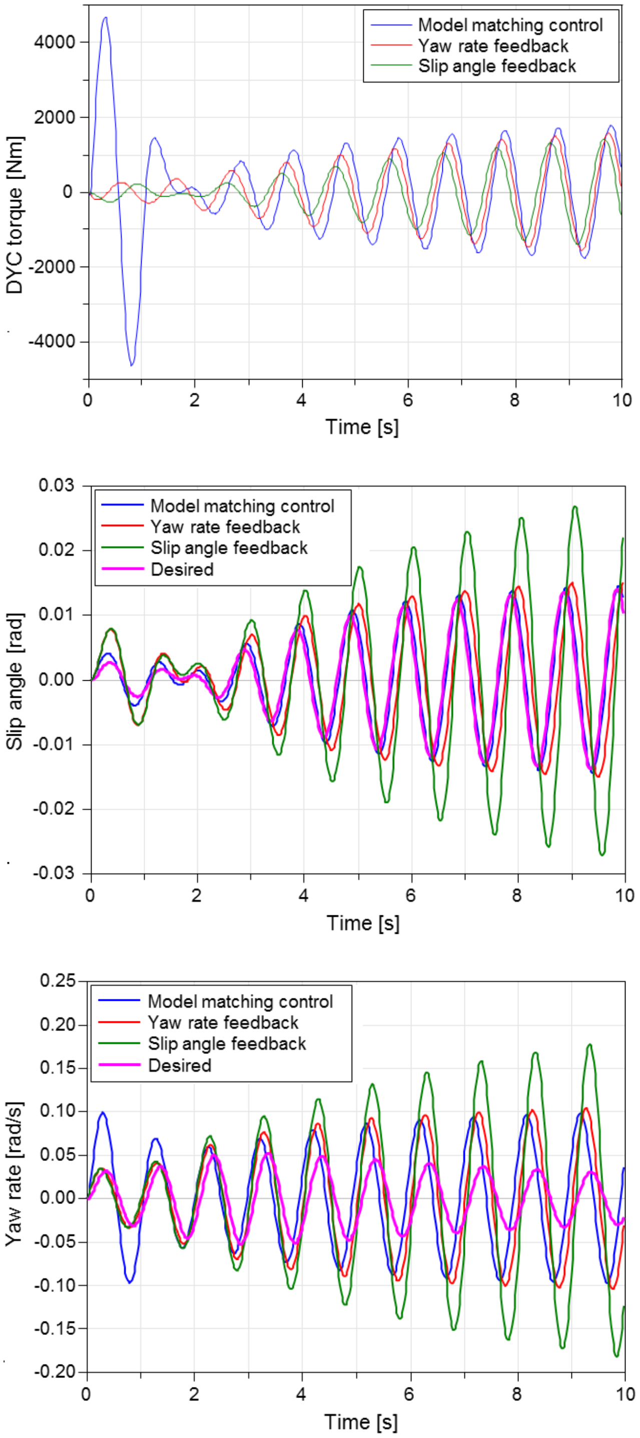

Figure 5. Simulation results by single track model

5 Simulation by Full Vehicle Model

5.1 Construction of the Full-Vehicle Model

The similar full vehicle model as previous research (Hirano, 2015) was used for full-vehicle simulation. The model was developed based on Vehicle Dynamics Library (Modelon, 2014) and was built as a full 3 dimensional (3D) multi-body-dynamic system (MBS) model. Component models of control systems such as TVD gearbox, electric motor and inverter were added with the full vehicle model. **Figure 7** shows the top level of the model hierarchy of the full vehicle test model and also the power train model with the controller.

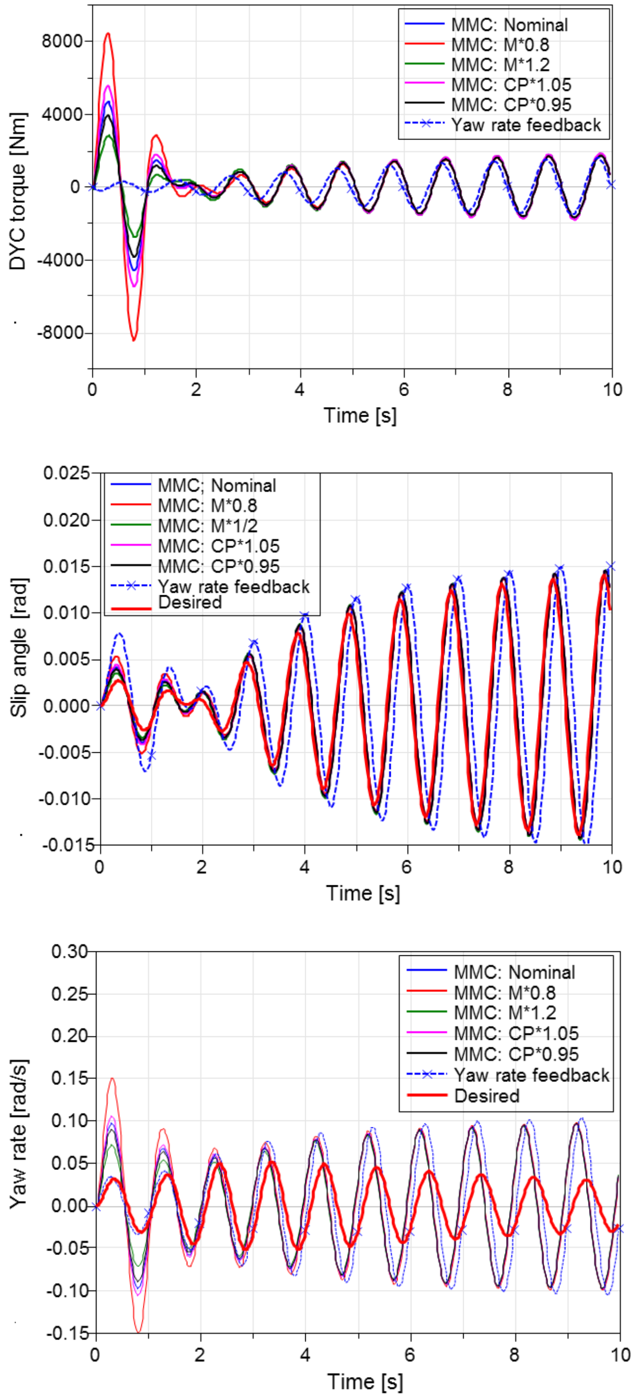

Figure 6. Robustness check by single track model

DOI 10.3384/ecp1612415

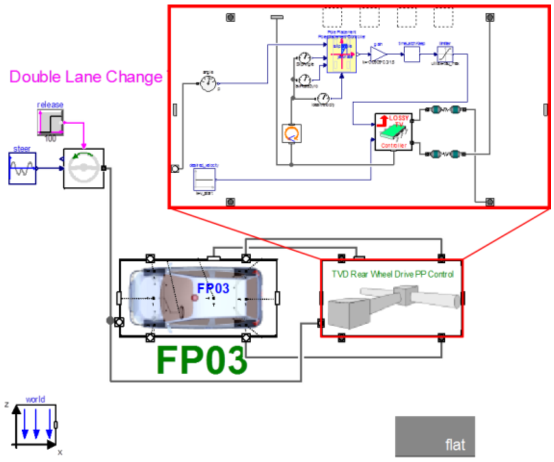

Figure 7. Structure of full vehicle test model

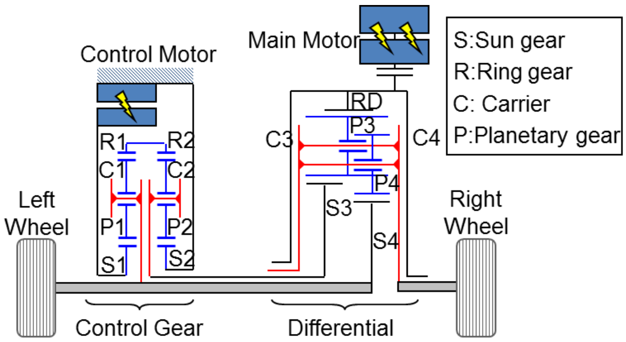

Figure 8. Torque vectoring differential (TVD) driveline

For the TVD gear train, a driveline structure referencing the MUTE project of the Technische Universität München (TUM) (Höhn et al., 2013) was selected. The TVD model was constructed using Power Train Library (DLR, 2013). **Figure 8** shows the configuration of the gear trains. Torque from the main motor is distributed equally to the left wheel and the right wheel through the differential gear. The torque distribution between the left wheel and the right wheel can be controlled by changing the torque input of the control motor.

3D MBS model of suspension, steering and body were installed to calculate vehicle dynamics characteristics. Suspension model was constructed as an assembled model of each suspension linkage, joints and force elements such as spring, damper and bushing. Non-linear tire model based on 'Magic Formula' model (Pacejka02) was used to calculate combined lateral force and longitudinal force of each tire. Steering model considered the characteristics of viscous friction of steering gear box and steering shaft as well as steering shaft stiffness. By these detailed models, it became possible to analyze the effects of steering angle change and camber angle change caused by vehicle roll, side force and tire aligning torque.

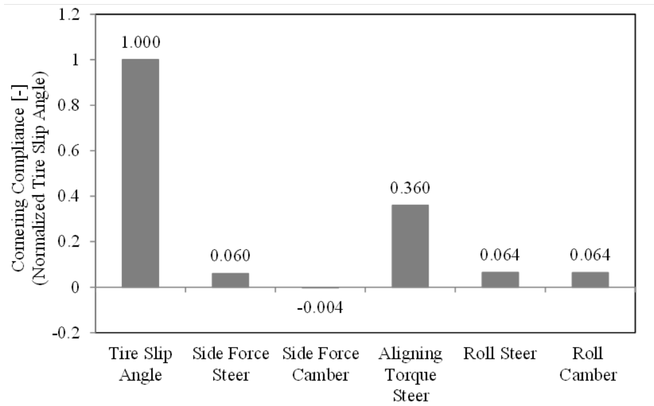

Figure 9. Effect of suspension characteristics to cornering compliance coefficient. (Normalized by the effect of tire slip angle.)

Figure 9 shows an analysis result about the effect of suspension characteristics to cornering compliance coefficient for an example of front double wish-born suspension. The coefficients are normalized by the effect of tire slip angle change. The equivalent cornering power coefficients were calculated by following equation.

$$\varepsilon_{f,r} = \frac{\frac{1}{C_{f,r}}}{\frac{1}{C_{f,r}} + \left\{ W_{f,r}\left(\frac{\partial\delta}{\partial F}\right)_{f,r} + W_{f,r}\left(\frac{\partial\gamma}{\partial F}\right)_{f,r}\frac{C_{s_{f,r}}}{C_{f,r}} + W_{f,r}\zeta_{f,r}\left(\frac{\partial\delta}{\partial M}\right)_{f,r} + \phi\left(\frac{\partial\delta}{\partial\phi}\right)_{f,r} + \phi\left(\frac{\partial\gamma}{\partial\phi}\right)_{f,r}\frac{C_{s_{f,r}}}{C_{f,r}} \right\}}$$

Here, C_f and C_r are the cornering power of tire itself. The terms in the curly brace of the denominator of the above equation indicates each effect shown in **Figure 9** respectively. Those are the effects by side force steer, side force camber, aligning torque steer, roll steer and roll camber respectively. Finally, the equivalent cornering power coefficients of front tires and rear tires were calculated as ε_f and ε_r respectively. These values are used to calculate the equivalent cornering power of each wheel shown in the equation (8) and equation (9) as bellows.

$$K_f = \varepsilon_f C_f$$

$$K_r = \varepsilon_r C_r$$

5.2 Results of Full Vehicle Simulation

Figure 10 shows the results of a double lane change test by the full vehicle model. Steering angle was given as a series of sinusoidal curves at a constant vehicle velocity of 100[km/h]. The model matching control showed better performance of tracking desired slip angle than the yaw rate feedback control. On the other hand, the yaw rate feedback control showed better performance for tracking the desired yaw rate, though this result can be expected naturally. Additionally, it became clear that the result of the vehicle motion by the model matching control was smoother than that by the PI yaw rate feedback control of desired yaw rate. The reason of this is assumed that feedforward part of model matching control works to improve the response. On the other hand, PI feedback control of the desired slip angle became unstable.

Figure 11 shows the result of full vehicle model simulation for the side wind test. Here, side wind of 20[m/s] blows while Time=2 [s] to 3.5 [s]. The vehicle runs at 120[km/h] and the steering wheel angle is kept to zero. Here, the similar result as the side wind test was obtained. The model matching control was good at tracking performance of the desired slip angle, and the PI feedback control of the desired yaw rate was good at tracking performance of the desired yaw rate. Also it is indicated that the control ability against steady deviation for the model matching controller is not enough. This indicates the necessity of modifying the model matching controller to introduce first order servo control by considering the integral of the error. Anyway both controls showed good performance of vehicle stabilization against the side wind than when no control was applied.

6 Conclusions

Model matching control of TVD was researched by using both linear single track model of vehicle dynamics and multi-physics large-scale full vehicle model. The following conclusions were obtained.

(i) Proposed model matching control showed a good performance especially for the tracking of the desired slip angle.

(ii) On the other hand, simple PI feedback control of desired yaw rate was good at tracking the desired yaw rate than the model matching control.

(iii) Improving the model matching controller to realize servo control of steady error deviation is necessary for future work.

Also for future work, the effect of drive shaft stiffness for TVD control should be investigated. More sophisticated control of tire slip and drive train oscillation should be researched also satisfying the requirement for the vehicle dynamics performance.

References

DLR, PowerTrain Library Users Guide (Version 2.1.0), 2013

Y. Hirano, S. Inoue and J. Ota, Model-based Development of Future Small EVs using Modelica, *Proceedings of Modelica Conference 2014*, 2014.

Y. Hirano, S. Inoue and J. Ota, Model Based Development of Future Small Electric Vehicle by Modelica, *Proceedings of Modelica Conference 2015*, 2015.

B. Höhn et al., Torque Vectoring Driveline for Electric Vehicle, *Proceedings of the FISITA 2012 World Automotive Congress*, Vol. 191, pp. 585-593, 2013.

Modelon, A.B., Vehicle Dynamics library Users Guide (Version 1.8), 2014.

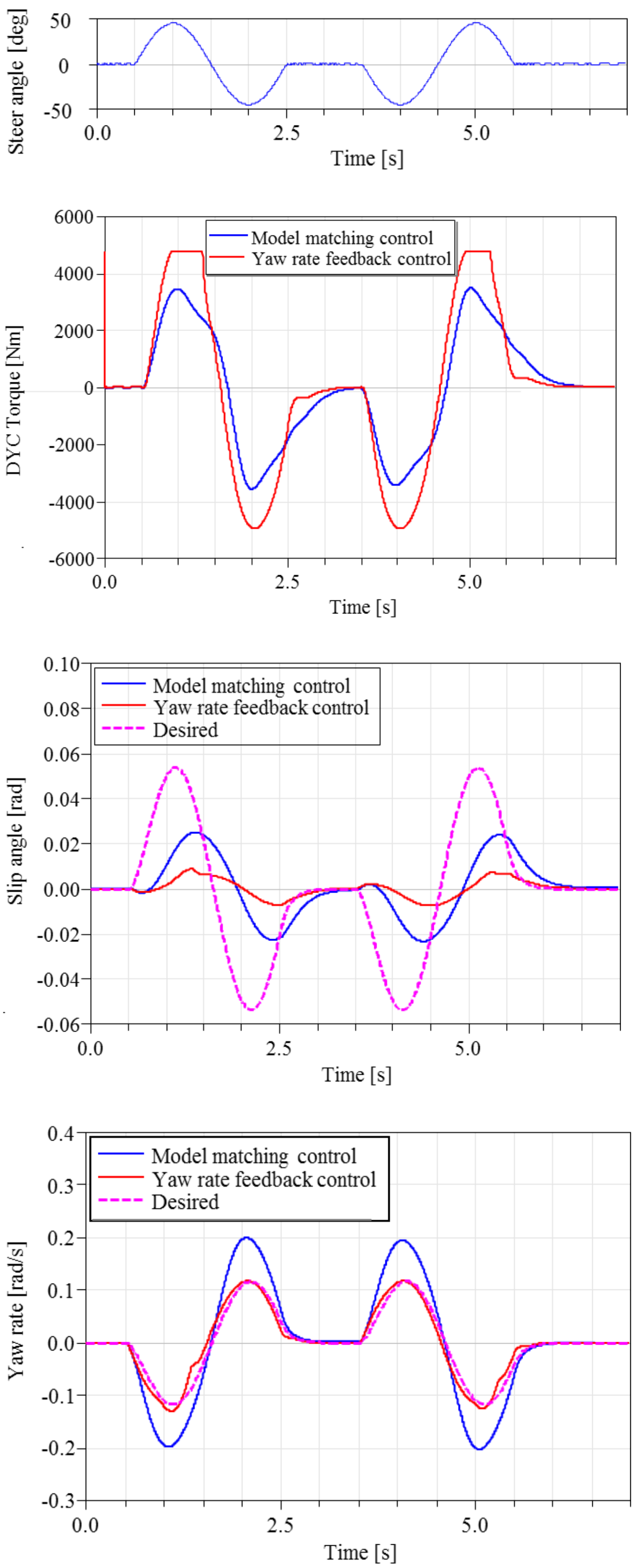

Figure 10. Simulation result of double lane change test by full vehicle model

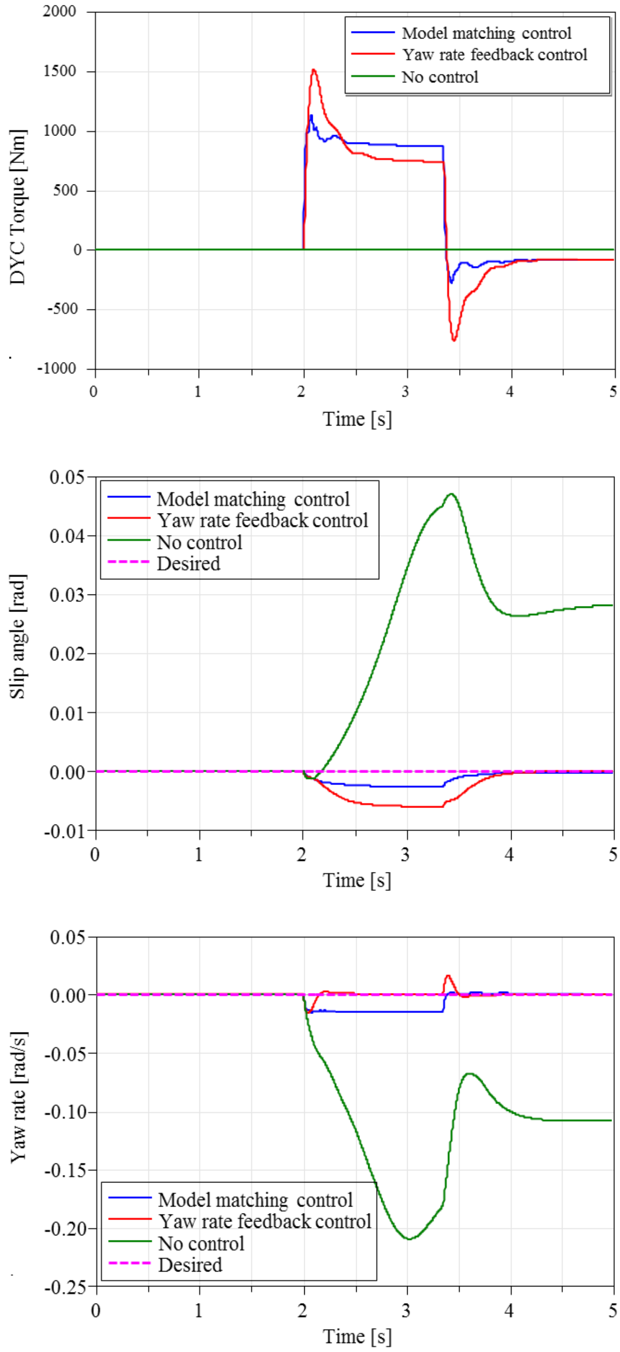

Figure 11. Simulation result of side wind test by full vehicle model